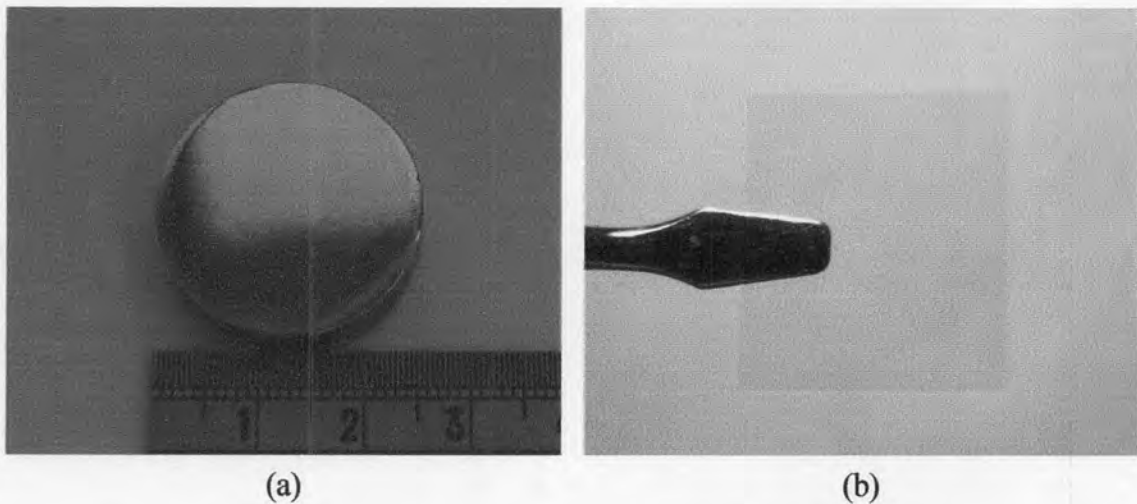


## CHAPTER III

### EXPERIMENTAL SETUP

#### 3.1 Samples

Three circular shape plates of stainless steel with a diameter of 25 mm were used as samples. These samples were well polished to make a good reflect of light. To prove an ability of optical coherence tomography (OCT), MENSEL-GLASER cover slide was also placed on the surface of these stainless steel plates. This cover slide had the refractive index of 1.5. The surface profile of each sample with and without cover slide was compared. The stainless steel plate and MENSEL-GLASER cover slide are shown in Figure 3.1.



**Figure 3.1:** Picture of (a) stainless steel plate and (b) MENSEL-GLASER cover slide

#### 3.2 Light Source and Controller

The 17.5 mW “Tow2” superluminescent diode (SLD) with mount from Superlum Ltd. was used as the low coherence light source in this research. Its central wavelength is 830 nm with 15 nm of full-width at half-maximum (FWHM) [22]. The +9V PILOT 2 controller was used to control and supply a current of the SLD light source. The “Tow2” SLD with mount is shown in Figure 3.2.

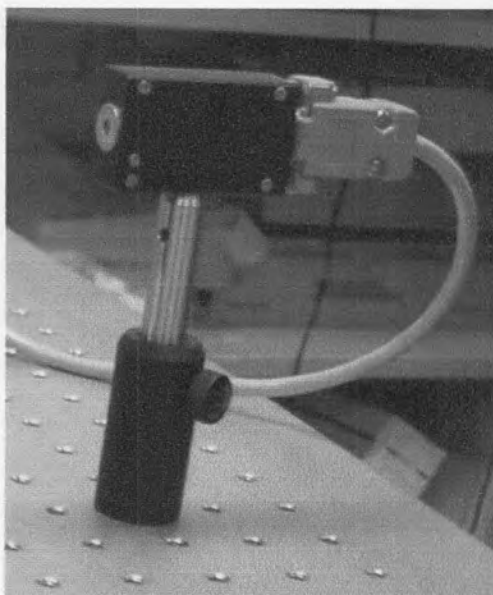


**Figure 3.2:** Picture of “Tow2” SLD with mount

### 3.3 Experimental Setup

In this research, the Michelson interferometer and the superluminescent diode (SLD) were used to characterize the surface profile of stainless steel samples. The experimental system was arranged as shown in Figure 3.3.

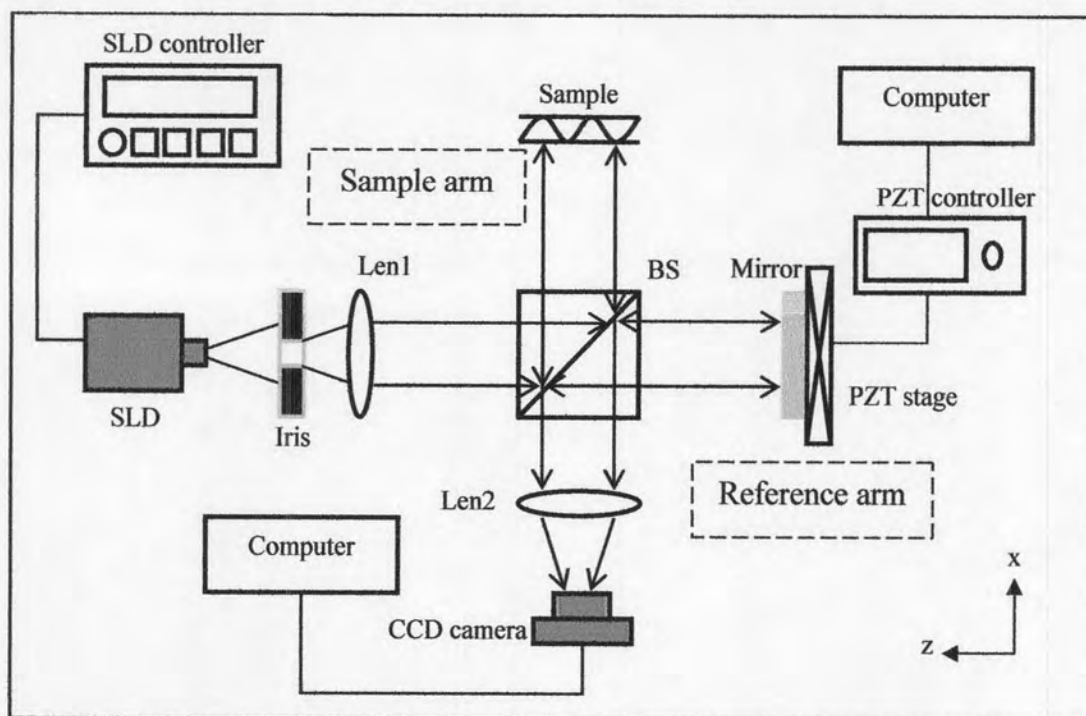


**Figure 3.3:** Setup for this experiment

The SLD generated a light beam, collimated by Len1. Then, this light beam was split into two arms; a reference arm and a sample arm, by beamsplitter (BS). Each beam reflected from the end of each arm, combined together and traveled to Len2. This combination beam contained path differences between two arms and then the interference patterns could be observed. In this research, SONY XCD-V50CR with  $640 \times 480$  pixels was used as CCD camera. It recorded intensity signal in every step of piezoelectric (PZT stage). Because the central wavelength of the SLD was 830 nm, a step of PZT stage was chosen as 100 nm ( $0.1 \mu\text{m}$ ) in order to obey the sampling theorem. A series of intensity signals in every step produced an interferogram; used to construct the surface profile of the samples. A peak position, which had a maximum intensity of the interferogram, was represented as a height of the surface.

In case a multi-layer material is used as the sample, the interference patterns can be observed when an equivalent of a position of the reference arm and a position of the layer is occurred. A number of interferograms, observed in this case, depends on a numbers of sample layers. For example, the sample of L layers can be produced L interferograms, as shown in Figure 3.4.

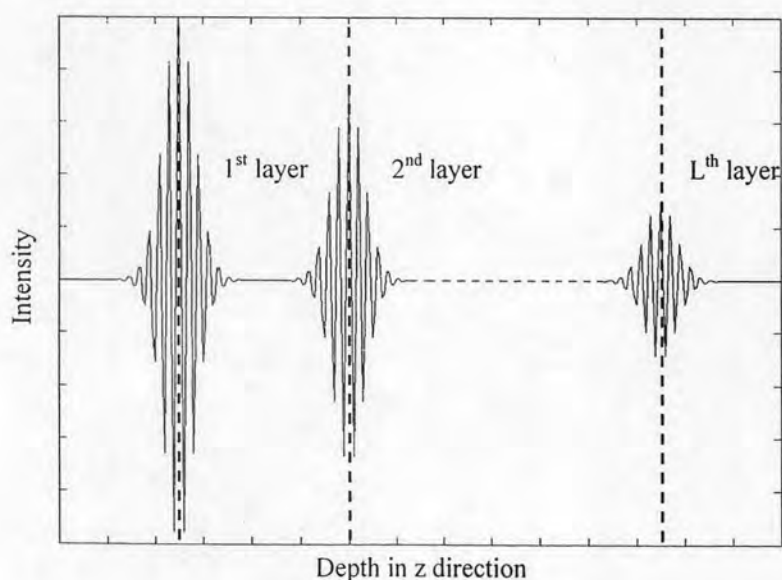


**Figure 3.4:** Interferogram of multi-layer sample

If the PZT stage is moved in  $z$  direction, the intensity at the CCD camera will be expressed by [10]:

$$\begin{aligned}
 I_D = & I_0 + I_0 V \exp\left[-\left(\frac{z-z_1}{l_c}\right)^2\right] \cos\left[\frac{4\pi(z-z_1)}{\bar{\lambda}}\right] \\
 & + I_0 V \exp\left[-\left(\frac{z-z_2}{l_c}\right)^2\right] \cos\left[\frac{4\pi(z-z_2)}{\bar{\lambda}}\right] \\
 & \quad \vdots \\
 & + I_0 V \exp\left[-\left(\frac{z-z_L}{l_c}\right)^2\right] \cos\left[\frac{4\pi(z-z_L)}{\bar{\lambda}}\right],
 \end{aligned} \tag{3.1}$$

where  $I_0$  is a background intensity,

$V$  is the fringe visibility,

$l_c$  is the coherence length of light,

$\bar{\lambda}$  is the central wavelength of light and

$z_L$  is a peak position of  $L^{\text{th}}$  layer.

To separate each layer, the coherence length of the light source must be less than the thickness of each layer. If the coherence length is wider than the thickness of each layer, the interferograms will be merged. Thus, information of some layers may be lost.

In this research, a parallel beam was used with the CCD camera. With this method, the parallel beam could be assumed that it was a set of small light sources. Each small light source produced the interferogram of a small area of the sample surface, which can be detected by each CCD pixel.

## 3.4 Experimental and Signal Analysis

### 3.4.1 Signal analysis process

A surface profile of the sample was constructed by analyzing interferograms. After the experimental apparatus was already set, backscattered intensity was recorded by CCD camera in each step of PZT stage along  $z$ -direction. The backscattered intensity of all step in each surface area, represented by each pixel of the CCD camera, was plotted as interferogram. Next, the interferogram was transformed by DFT to spatial domain.

A noise in this interferogram was also reduced by using the Butterworth window in a digital filtering method. The interferogram in frequency domain was again transformed to time domain and then a position in z-direction, which had maximum intensity, was calculated from this inverse interferogram. The position in each surface area represented a surface height of the select area.

For more accuracy of the surface height, the noise-reducing interferogram was analyzed by CWT with the Morlet wavelet, used as the mother wavelet. The time-frequency spectrogram was constructed and the maximum point of this spectrogram was defined. By using a maximum point of the CWT spectrogram and the phase of this point, the surface height in z-direction could be solved by Eq.(2.32). The diagram of a signal analyzing process is shown in Figure 3.5.



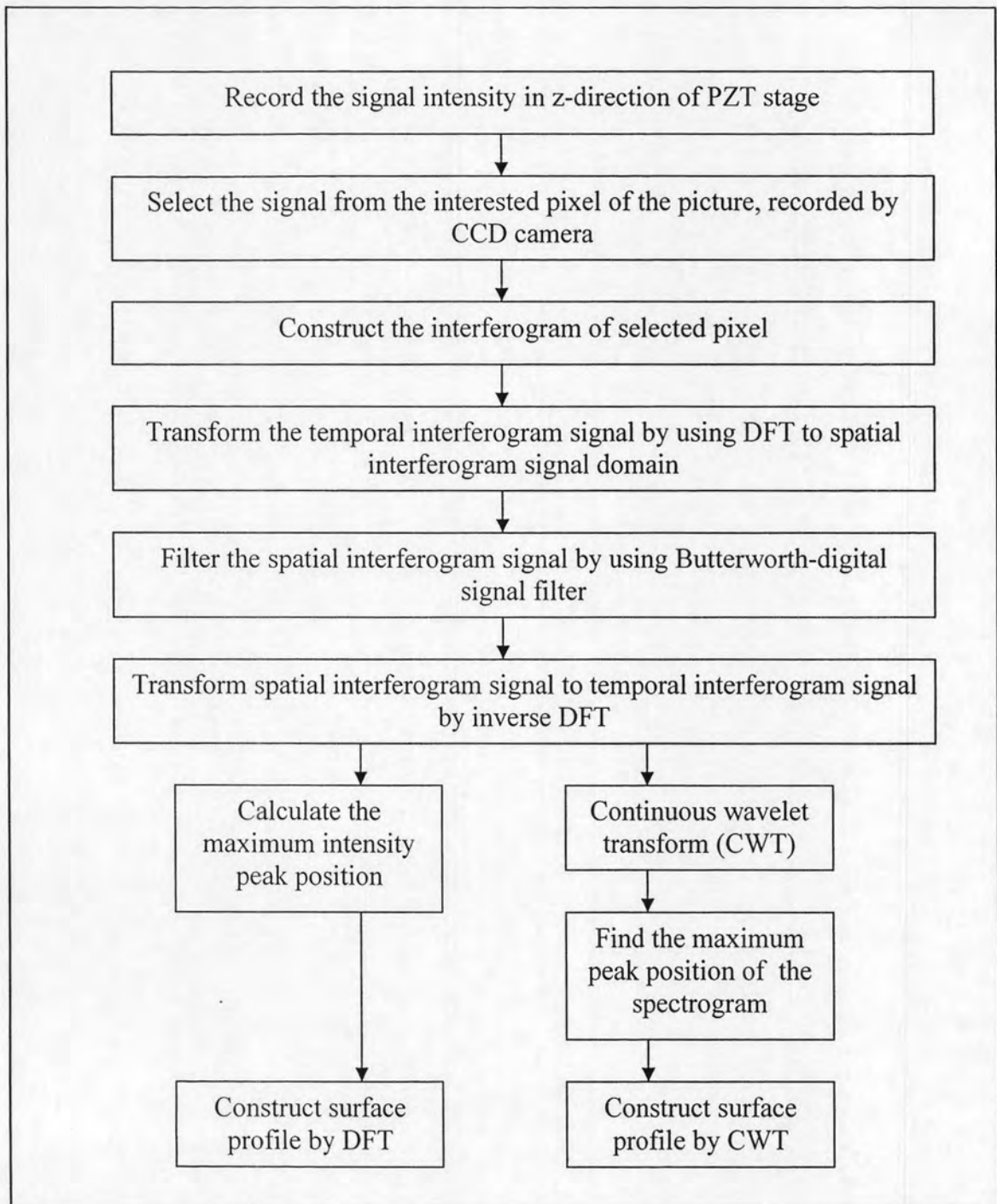


Figure 3.5: Signal analyzing diagram

### 3.4.2 Coherence length measurement

As the coherence length is a key to define a resolution of the surface height, the coherence length of the SLD, used in this research, was first parameter to measure. For specifying the coherence length, interferogram of a plain mirror was constructed by stepping  $0.1 \mu\text{m}$  in  $z$ -direction of the PZT stage. This interferogram was analyzed by the DFT, digital filtering and inverse DFT, respectively.

### 3.4.3 Discrete Fourier transform and continuous wavelet transform comparing

To compare a resolution by using DFT and CWT, a surface profile of step-height standard plate, which its cross-section is shown in Figure 3.6, was tested by both methods. A depth in  $z$ -direction of a top and bottom surface was calculated. To confirm the surface profile constructing ability, 3-D surface profile of this step-height standard plate would be constructed. To avoid an effect of a reflected light from neighbor CCD pixel, the surface profile of this step-height standard plate in each area was constructed by an average of  $4 \times 4$  pixels.

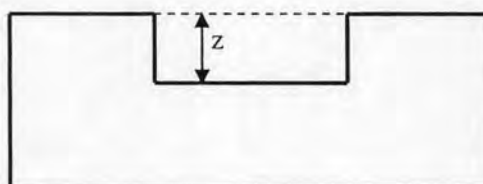


Figure 3.6: Cross-section of step-height standard plate

Next, an efficiency of DFT and CWT was also compared by a cross-section of three stainless steel plates. A root-mean-square roughness ( $R_q$ ) was also calculated in each stainless steel plate and the results were compared with  $R_q$  from 3-D Non-Contact Surface Profiler SP-500 Series from Toray Engineering Co., Ltd, which was used as standard instrument. This standard instrument was used focused beam method, phase shift algorithm and the Michelson interferometer.

### **3.4.4 Surface profile construction**

A possibility of CWT to construct a surface profile with and without transparent cover was studied. The surface profiles of three stainless steel plates with and without the cover slide were constructed and  $R_q$  from covered and uncovered surface were compared.

### **3.4.5 Application of OCT with the CWT by measuring the thickness of transparent material**

The SLD had low intensity, interference patterns from a transparent material surface was so weak to be detected by CCD camera. Thus, a thickness of transparent material could be measured by comparing the interferogram of the sample surface without cover surface and the one with transparent cover. When the surface was covered by the transparent material, the observed depth position was deeper than the real one due to an effect of the refractive index of the transparent material. In this research, the thickness of the transparent material was calculated by finding differences of depth between uncovered surface and covered surface. The real thickness of the transparent material was calculated by dividing this different value with the refractive index, as expressed in Eq.(2.32). The calculated real thickness was compared with the one, measured by length measuring instrument ULM RUBIN 800 from MAHR METROLOGY that used force compression method.